ISSN 0915-633X

# NATIONAL INSTITUTE FOR FUSION SCIENCE

## Collisionless Driven Reconnection in an Open System

R. Horiuchi, W. Pei and T. Sato

(Received - June 16, 2000)

NIFS-637 June 2000



RESEARCH REPORT
NIFS Series

NAGOYA, JAPAN

# Collisionless Driven Reconnection in an Open System

Ritoku Horiuchi[1,2], Wenbing Pei[2], and Tetsuya Sato[1,2]

[1] *National Institute for Fusion Science, Toki 509-5292, Japan*
[2] *The Graduate University for Advanced Studies Toki 509-5292, Japan*

**abstract**

Particle simulation studies of collisionless driven reconnection in an open system are presented Collisionless reconnection evolves in two steps in accordance with the formation of two current layers, i.e., an ion current layer in the early ion phase and an electron current layer in the late electron phase. After the electron current layer is formed inside the ion current layer, the system relaxes gradually to a steady state when convergent plasma flow is driven by an external electric field with a narrow input window. On the other hand, when the convergent plasma flow is driven from the wide input window, magnetic reconnection takes place in an intermittent manner, due to the frequent formation of magnetic islands in the vicinity of neutral sheet.

KEYWORDS: collisionless driven reconnection, open system, anomalous resistivity, particle kinetic effect, particle simulation

## 1. Introduction

Collisionless magnetic reconnection plays an essential role in energetic active phenomena observed in the solar corona (Priest, 1982), the Earth's magnetosphere (Nishida, 1978) and the laboratory plasma (Ono *et al.*, 1996). In most situations the system is open and evolves dynamically with time. Therefore, microscopic kinetic process of collisionless reconnection is deeply connected with the dynamical evolution of a whole system. By making use of two-dimensional particle simulation for an open system, Horiuchi and Sato (1994,1997) have examined the kinetic process and have clarified that nonlinear evolution of collisionless reconnection is controlled not only by an internal microscopic process such as an electron dynamics or an ion dynamics in a current sheet, but also by an external global condition such as energy input rate or external driving flow. However, these analyses are restricted to the initial growing phase of collisionless driven reconnection because a periodic boundary condition is used at the downstream boundary.

Magnetic reconnection is often discussed with steady models. On the other hand, long time scale MHD simulations (Kitabata *et al.*, 1996, Amo *et al.*, 1995) have demonstrated that magnetic reconnection takes place intermittently when there exists a constant energy supply from the exterior region Which situation is realized in collisionless reconnection ? It is believed that steady reconnection is realized when the flux input rate into the system is balanced with the reconnection rate. However, this balance condition is not always assured because magnetic reconnection is controlled by two different processes with different time scales, i.e., an external global process and an internal microscopic process In order to study a long time scale behavior of collisionless driven reconnection we developed a new open boundary model in which a free condition is used at the downstream boundary. By making use of both two-dimensional and three-dimensional kinetic open models, we will discuss the dynamics of collisionless driven reconnection in an open system that is subject to an external driving source.

## 2. Simulation Model

Three different types of electromagnetic particle codes are developed for the analyses of collisionless driven reconnection in two-dimensional and three-dimensional Cartesian coordinate systems (Horiuchi and Sato, 1994, 1997, 1999). As an initial condition we adopt a one-dimensional equilibrium with the Harris-type anti-parallel magnetic configuration as

$$\mathbf{B}(y) = (B_x(y), 0, 0) \tag{1}$$

$$B_x(y) = B_0 \tanh(y/L), \tag{2}$$

$$P(y) = B_0^2/8\pi \ \mathrm{sech}^2(y/L), \tag{3}$$

where $B_0$ is a constant and $L$ is the scale height along the y-axis. There is a magnetically neutral sheet at $y = 0$ in the initial equilibrium. The initial particle distribution is assumed to be a shifted Maxwellian with spatially constant temperature and average particle velocity, which is equal to the diamagnetic drift velocity

The same input condition is used at the upstream boundary so that the plasma inflows are symmetrically driven from two input boundaries ($y = \pm y_b$) by the external electric fields imposed in the z direction. The amplitude of driving field $E_{zd}(x,t)$ is set for zero at $t = 0$, and increases with time while keeping a bell-shaped profile near the center and a flat profile in the periphery for an initial short moment. After then a constant profile is kept with maximum flux input rate $E_0$. Two types of boundary conditions are considered

at the downstream boundary ($x = \pm x_b$), i.e., (a) a periodic boundary condition, and (b) a free boundary condition. For the free boundary case field quantities are assumed that $E_x$, $E_y$ and $\partial E_z/\partial x$ are continuous at $x = \pm x_b$. The boundary condition for particles is determined so as to keep the charge neutrality condition and the net number flux of particles associated the fluid velocity in the vicinity of the downstream boundary. In this open model the total number of particles is a function of time.

## 3. Two-step evolution of collisionless driven reconnection

In this section we review briefly the results of two-dimensional particle simulation for the open model with the periodic downstream boundary (Horiuchi and Sato, 1994, 1997). Charged particles execute a complex thermal motion, which is called a meandering motion, in the vicinity of magnetically neutral sheet. The orbit amplitude of meandering motion is given by the geometrical mean of Larmor radius and the scale height of magnetic field. When there exists an external driving source, the current sheet evolves dynamically with time. That is, physical parameters, which control collisionless reconnection, becomes a function of time. In considering collisionless reconnection in the presence of an external driving source, it is important to examine the temporal evolution of physical parameters and their relationship.

Figures 1 and 2 show (1) the temporal evolution of an electric field along equilibrium current at the reconnection point ("reconnection electric field" ), and (2) those of four spatial scales for the case of $m_i/m_e = 50$ and $E_0 = -0.04B_0$, where $t_A$ is the Alfven transit time, $d_h$, $d_{jz}$, $l_{mi}$, and $l_{me}$ are the half-width of the mass density profile, that of the current density profile, the average amplitude of ion meandering orbit, and that of electron meandering orbit, respectively. Figure 1 indicates that collisionless reconnection takes place in two steps, i.e., the slow reconnection in the early phase ( $0.6t_A < t < 1.3t_A$ ) and the fast reconnection in the late phase ( $1.3t_A < t < 1.8t_A$ ). The electric field begins to grow slowly as soon as both $d_h$ and $d_{jz}$ start decreasing as a result of the compression by the convergent plasma flow in the slow reconnection phase. The width of the current layer is almost the same or a little larger than the ion thermal scale $l_{mi}$ in this phase.

Because most of the ions are unmagnetized in the current layer ( " ion current layer " ) while the electrons are magnetized, the input flow ( Poynting flux ) no longer works on thinning the ion current layer, but it continues to compress the electron profile. Thus, electron current layer is created inside the ion current layer due to the finite ion Larmor radius effect. When the fast reconnection phase sets in, the inclination of the growth curve steepens suddenly and the half-width of electron current layer approaches the electron thermal scale $l_{me}$. These results lead us to the conclusion that the slow reconnection is triggered by the ion meandering motion effect while the fast reconnection is triggered by the electron meandering motion effect.

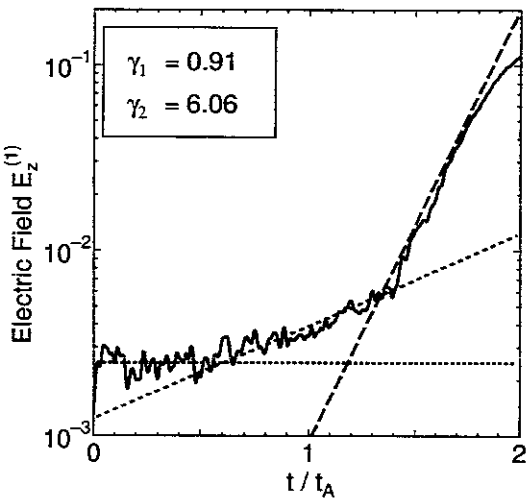


Fig. 1. Temporal evolution of reconnection electric field for the case of periodic downstream boundary.

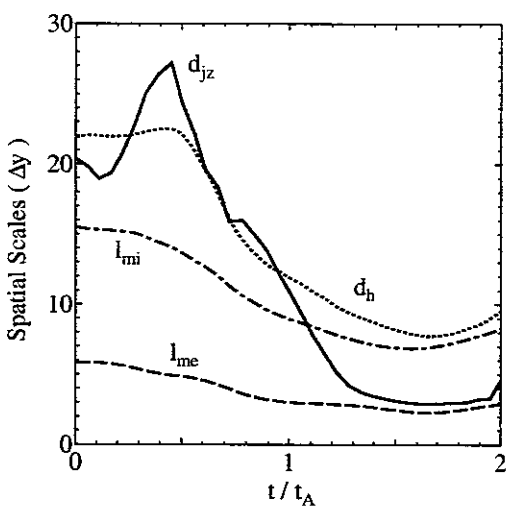


Fig. 2. Temporal evolutions of four spatial scales for the case of periodic downstream boundary.

From the simulation runs with a various values of ion mass, electron mass, and the driving electric field (Horiuchi and Sato, 1994, 1997), it is found that the fundamental properties of collisionless driven reconnection are determined by two physical processes, i.e., the external process which controls the flux input rate into the current layer, and the internal process which controls the particle kinetic mechanism leading to collisionless driven reconnection in the current layer, and they are not independent processes but deeply connected to each other.

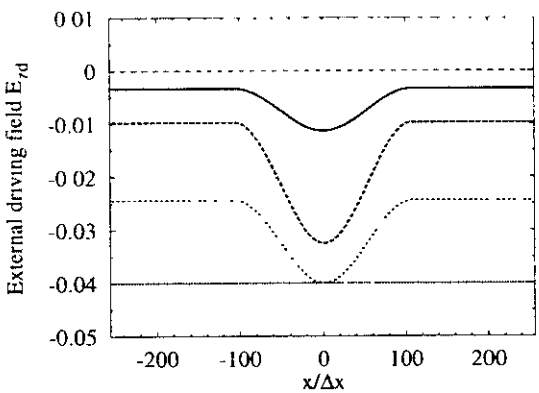


Fig. 3 Spatial profiles of driving electric field at five different time periods for the case of $x_d = 0.84x_b$ and $E_0 = -0.04B_0$.

## 4. Dynamics of collisionless reconnection in a long time scale

In this section we discuss the particle simulation in a long time scale based on the two-dimensional open model with the free downstream boundary. The simulation is carried out on a 512 × 128 point grid by making use of 6.4 million particles. The main parameters are in the followings: $m_i/m_e = 25$, $\omega_{pe}/\omega_{ce} = 3.5$, $\omega_{ce}\Delta t = 0.02$, $L = 0.8y_b \approx 3\rho_i$, where $\rho_i$ is the ion Larmor radius. Figure 3 shows the spatial profiles of the driving electric field imposed at the input boundary at five different time periods, i.e., $t\omega_{ce} = 0$, 10.2, 20.4, 81.6, and 143. Here, the spatial size of initial bell-shaped profile is $x_d = 0.84x_b$, and the amplitude of the uniform profile in the late phase is $E_0 = -0.04B_0$. We call the parameter $x_d$ input window size, because the input velocity is locally enhanced within this region. In order to examine the dependence of the reconnection process on the profile of driving electric field, we performed simulation runs with fixed $E_0$ and varying $x_d/2x_b$ (=0.42, 0.62, 0.83).

First, let us consider the case of narrow input window ( $x_d/2x_b = 0.42$ or $x_d = 18\rho_i$ ) Figure 4 shows the temporal evolution of the magnetic field. The convergent flow supplied from the top and bottom boundaries compresses the current sheet. Magnetic reconnection sets in at the center of the simulation domain at $t\omega_{ce} \approx 122$ (second panel). A small island appears near the reconnection point and grows with time (third panel). After some periods this island disappears due to the merging with right bulk plasma. Any magnetic island is not created ever after and so global field topology remains unchanged. That is, the system reaches a steady reconnection state.

Figure 5 plots the time history of an electric field at the reconnection point for the same case as Fig. 4 where the dotted line stands for the value of driving electric field. The behavior of the reconnection field for an initial growing phase is very similar to the simulation results discussed in Sec. 3. After over-shooting the

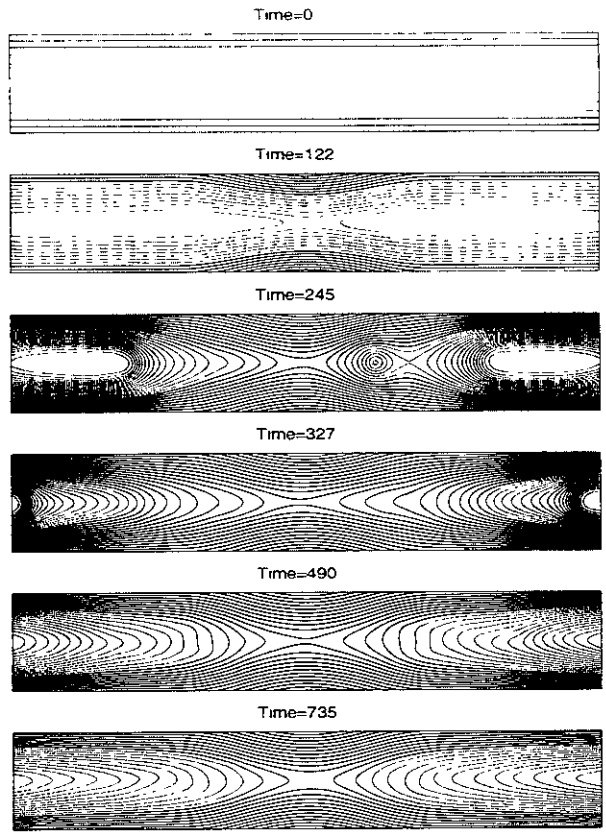


Fig. 4. Temporal evolution of magnetic field for the narrow window case of $x_d/2x_b = 0.42$

field approaches the external driving field. The reconnection field tends to fluctuate around the value of the external field with a small amplitude for $t\omega_{ce} > 300$. Figure 6 is the time history of three spatial scales. The width of current layer approaches the electron meandering scale $l_{me}$ for an initial growing phase in accordance with the formation of the electron current layer. However, it tends to increase for $t\omega_{ce} > 160$ and is kept nearly equal to the ion meandering scale $l_{mi}$ in a steady state. The electron current density is described by the superposition of an electron density profile and an average electron velocity profile. The electron density profile has an ion scale because it takes almost the same form as the ion density profile. On the other hand, the electron velocity profile, which has an electron scale, is strongly dependent on the acceleration mechanism in the electron current layer. If a locally enhanced profile of average electron velocity is formed, the electron current layer is clearly visible inside the ion current layer. Figure 6 suggests that the localized peaked profile of electron velocity formed in the initial growing phase is damped down and the electron current layer becomes invisible in the steady state.

Now, let us discuss the simulation results for the wide window case ( $x_d/2x_b = 0.83$ or $x_d = 36\rho_i$ ) Figure 7 illustrates the spatial profile of magnetic field at ten

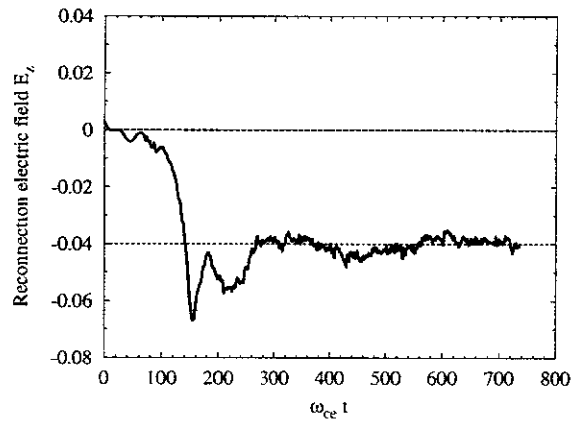


Fig. 5. Temporal evolutions of reconnection electric field for the narrow window case of $x_d/2x_b = 0.42$.

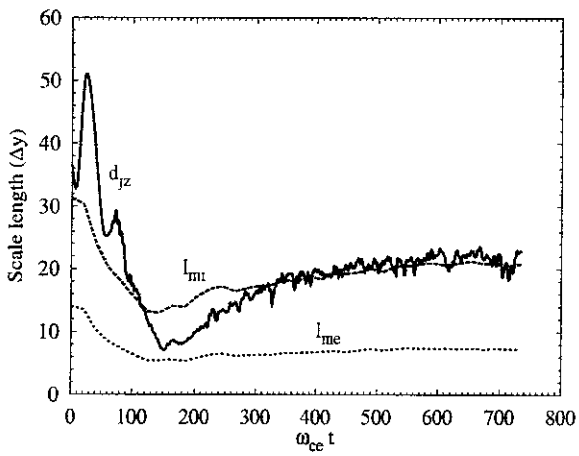


Fig. 6. Temporal evolutions of three spatial scales for the narrow window case of $x_d/2x_b = 0.42$.

different time periods. A small island is created at the center of current sheet at $t\omega_{ce} = 143$. This island grows with time while moving to the left. The system relaxed to a state without any island after this island moves out through the left boundary ( $t\omega_{ce} = 429$ ). After a short period a small island is created again at the center at $t\omega_{ce} = 572$. This island moves to the right while increasing its size and disappears through the right boundary. This process is repeated again and again. An elongated current sheet along the x-axis is created as a result of the plasma compression over a relatively long range for the wide window case. The length of the current sheet is roughly estimated as $L_{cs} \approx 10\rho_i$. This means that the current sheet becomes unstable against a collisionless tearing instability. Consequently, the system cannot reach any steady state due to the frequent formation of magnetic islands in the current sheet. Figure 8 plots the temporal evolution of the reconnection electric field for the same case as Fig. 7. One can see

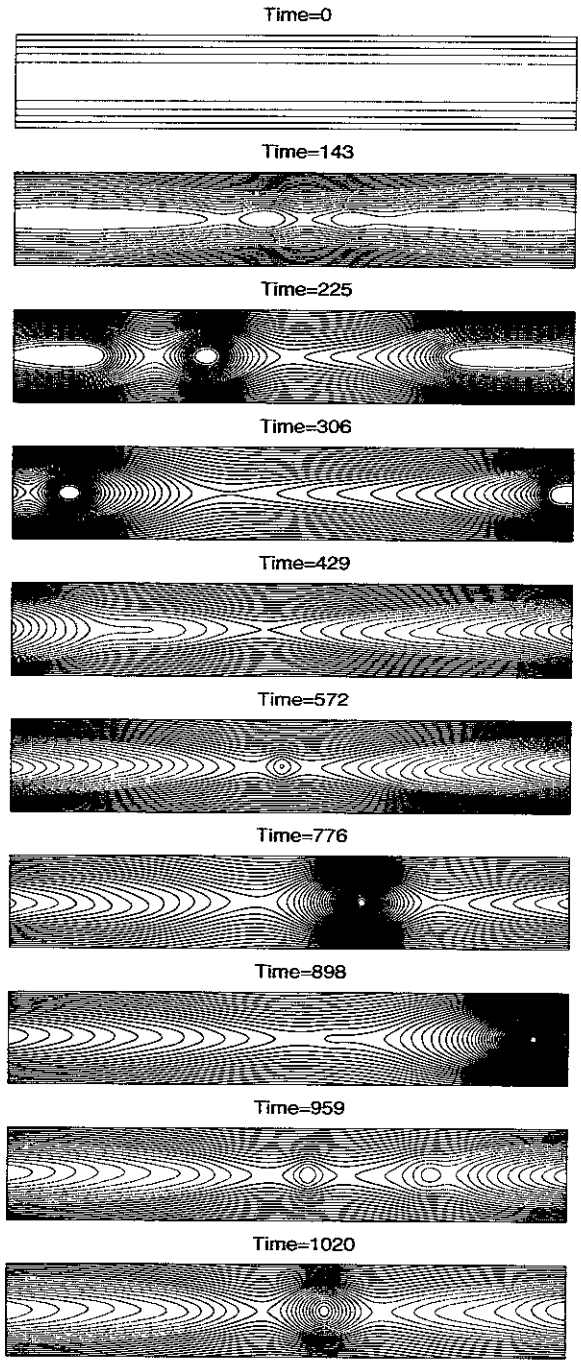


Fig. 7. Temporal evolutions of magnetic field for the wide window case of $x_d/2x_b = 0.83$.

in Fig. 8 that, compared with the narrow window case, the reconnection field is fluctuating around the value of the external field with a relatively larger amplitude during the simulation, and never reaches a constant value. It is concluded that, for wide window case, collisionless reconnection takes place intermittently, but not in a steady way.

We can see another interesting phenomenon of an

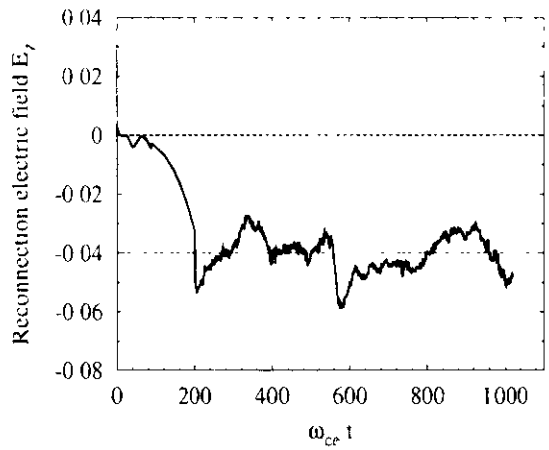


Fig 8 Temporal evolutions of reconnection electric field for the wide window case of $x_d/2x_b = 0\ 83$

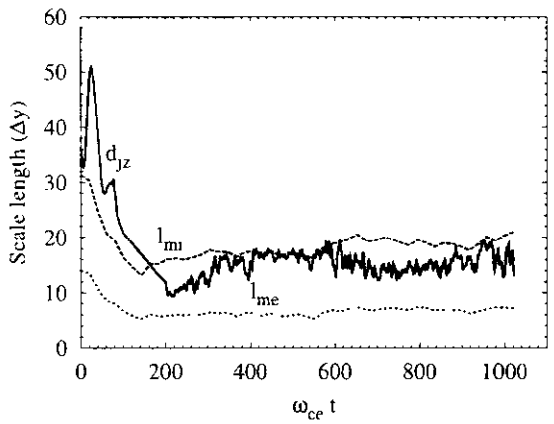


Fig 9 Temporal evolutions of three spatial scales for the wide window case of $x_d/2x_b = 0.83$.

intermittent reconnection in Fig. 9. The width of the current layer $d_{jz}$ changes between the ion scale $l_{mi}$ and the electron scale $l_{me}$ in accordance with the fluctuation of the reconnection electric field. When the reconnection field exceeds the driving field, the width decreases below $l_{mi}$ and the electron current layer becomes visible inside the ion current layer. It is interesting to note that this period corresponds to the growing phase of magnetic islands in the neutral sheet On the other hand, when the reconnection field has a value close to the driving field, the width returns to $l_{mi}$ and the electron current layer becomes invisible. In this way, collisionless reconnection takes place intermittently while changing the spatial structure of the current sheet dynamically for wide window case.

## 5. Collisionless driven reconnection in three dimensions

Horiuchi and Sato (1999) have demonstrated that, for no external driving source, two different types of plasma instabilities are excited in three-dimensional current layer The lower hybrid drift instability (Krall and Liewer, 1971) is observed to grow in the periphery of current layer in an early period, while a drift kink instability (DKI) (Daughton, 1998) is triggered at the neutral sheet in a late period as a result of the nonlinear deformation of the current sheet by the lower hybrid drift instability A reconnection electric field grows at the neutral sheet in accordance with the excitation of the DKI Collisionless reconnection is terminated for a relatively short period in the absence of an external driving field because the total amount of magnetic flux available for magnetic reconnection is limited Thus, the magnetic flux supply from the exterior region is needed for the continuation of collisionless reconnection.

Let us examine how collisionless reconnection evolve in three dimensions in the presence of an external driving source. The three-dimensional particle simulation is carried out on a $128 \times 64 \times 64$ point grid by making use of 24 million particles for the open model in which the periodic condition is adopted at the boundary of the x-axis ( $x = \pm x_b$ ) and that of the z-axis ( $z = \pm z_b$ ), and the input condition is used at the boundary of the y-axis ( $y = \pm y_b$ ). Figure 10 shows the temporal evolutions of the Fourier amplitude of the drift kink mode (solid), the reconnection electric field (dashed), and the half-width of the current layer (dotted) for the case of $m_i/m_e = 100$ and $E_0 = -0\ 02B_0$ The Poynting flux, which is supplied into the simulation domain from the exterior region, moves towards the current layer together with the convergent plasma flow, while compressing the current profile. The compression by the convergent plasma flow increases the growth rate of the DKI Because most of ions inside the current layer are unmagnetized, the electric field or the Poynting flux, which is carried by the convergent plasma motion, penetrates into the current layer due to the particle kinetic effect (Horiuchi and Sato, 1994, 1997) When the Poynting flux reaches the neutral sheet, collisionless reconnection is triggered by the convective electric field

Once magnetic reconnection takes place, a generated fast plasma flow carries away the plasma near the reconnection point towards the downstream. One can see in Fig 10 that, after the reconnection electric field reaches its saturation level, the amplitude of the DKI decreases and the width of the current layer increases. These phenomena indicate that the reconnection flow carries away the plasmas faster than the flux is accumulated at the reconnection point by the input flow Consequently, the current profile is flattened in the vicinity of the reconnection point and the DKI becomes stable there. Figure 11 shows the perspective views of the current sheet at $t\omega_{ce} = 408$ in the (x,y,z) space for the same case as Fig. 10 Reconnection point appears almost along the straight midline ( $x = 0$ ) in the current sheet ( see a green color in the central region) We cannot see any modification of the current sheet by the DKI in the vicinity of reconnection point although

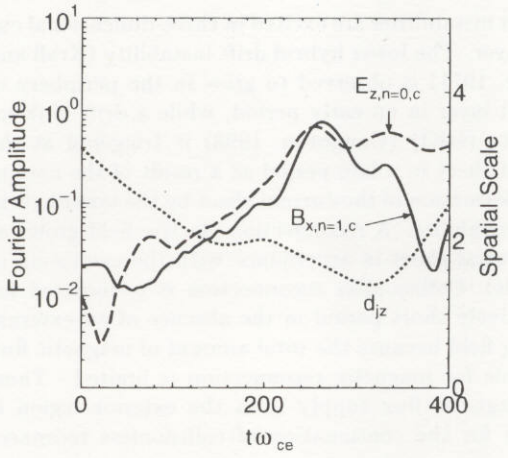


Fig. 10. Temporal evolutions of the Fourier modes and the half-width of current layer for the three-dimensional simulation where the solid, dashed, and dotted lines stand for the drift kink mode, the reconnection electric field, and the half-width, respectively.

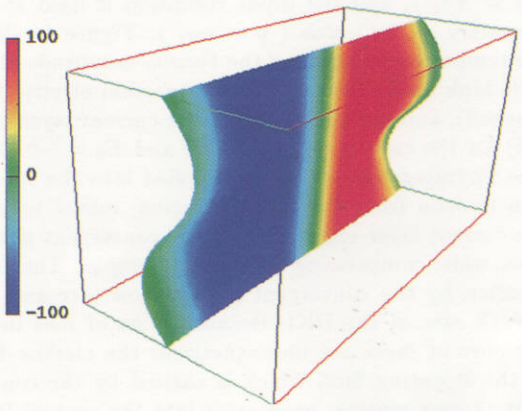


Fig. 11. Perspective views of the current sheet at $t\omega_{ce} = 408$ for the same case as Fig. 10 where the current sheet is defined by the condition $B_x = 0$, red and blue colors stand for the positive and negative values of magnetic field $B_y$.

there appears the $n = 1$ modification of the current sheet along the z-axis in the downstream region. It is concluded that the drift kink instability is not a primary cause of collisionless reconnection in the presence of an external driving source.

## 6. Summary

Based on two-dimensional and three-dimensional kinetic models, we have investigated the dynamics of collisionless driven reconnection in an open system that is subject to an external driving source.

It is found from two-dimensional kinetic simulations with the periodic downstream boundary that collisionless reconnection evolves in two steps in accordance with the formation of two current layers, i.e., an ion current layer in the early phase and an electron current layer in the late phase. The slow reconnection in the early phase is triggered by the ion meandering motion effect while the fast reconnection in the late phase is triggered by the electron meandering motion effect.

A long time scale behavior of collisionless reconnection is investigated by using two-dimensional open model with the free downstream boundary. When the convergent plasma flow is driven by an external electric field with a narrow input window ($x_d = 18\rho_i$), the system relaxes to a steady state in which the reconnection rate is determined by the external electric field. On the other hand, when the input window is wide ($x_d = 36\rho_i$), magnetic reconnection takes place in an intermittent manner due to the frequent formation of magnetic islands in the neutral sheet.

The relationship between the anomalous resistivity associated with wave-particle interaction and collisionless reconnection has been investigated by means of three-dimensional particle simulation for an open system. It is found that the drift kink instability, which is excited through the compression of current sheet by the divergent plasma flow in the early phase, is stabilized by the reconnection flow after magnetic reconnection is fully developed. Thus, a primary cause of collisionless reconnection is not the drift kink instability, but the particle kinetic effect in the presence of an external driving source.

## References


H. Amo, T. Sato, A. Kageyama, K. Watanabe, R. Horiuchi, T. Hayashi, Y. Todo, T. H. Watanabe, and H. Takamaru, Phys. Rev., **E51**, 3838-3841, 1995.

W. Daughton, J. Geophys. Res., **103**, 29429-29443, 1998.

R. Horiuchi and T. Sato, Phys. Plasmas, **1**, 3587-3597, 1994.

R. Horiuchi and T. Sato, Phys. Plasmas, **4**, 277-289, 1997.

R. Horiuchi and T. Sato, Phys. Plasmas, **6**, 4565-4574, 1999.

N. A. Krall and P. C. Liewer, Phys. Rev., **4**, 2094-2103, 1971.

H. Kitabata, T. Hayashi, T. Sato, R. Horiuchi, K. Watanabe, A. Kageyama, T. H. Watanabe, Y. Todo, and H. Takamaru, J. Phys. Soc. Japan, **65**, 3208-3214, 1996.

A. Nishida, *Geomagnetic Diagnostics of the Magnetoshpere* (Springer-Verlang, New York, 1978), p. 38.

Y. Ono, M. Yamada, T. Akao, T. Tajima, and R. Matsumoto, Phys. Rev. Lett. **76**, 3328(1996).

E. R. Priest, *Solar Magnetohydrodynamics* (Dordrecht,Reidel,1982).

## Recent Issues of NIFS Series

NIFS-570 T Hayashi, N. Mizuguchi, T-H Watanabe, T Sato and the Complexity Simulation Group,
*Nonlinear Simulations of Internal Reconnection Event in Spherical Tokamak*, Oct 1998
(IAEA-CN-69/TH3/3)

NIFS-571 A. Iiyoshi, A. Komori, A. Ejiri, M. Emoto, H. Funaba, M. Goto, K. Ida, H. Idei, S. Inagaki, S. Kado, O. Kaneko, K. Kawahata, S. Kubo, R. Kumazawa, S. Masuzaki, T. Minami, J. Miyazawa, T. Morisaki, S. Morita, S. Murakami, S. Muto, T. Muto, Y. Nagayama, Y. Nakamura, H. Nakanishi, K. Narihara, K. Nishimura, N. Noda, T. Kobuchi, S. Ohdachi, N. Ohyabu, Y. Oka, M. Osakabe, T. Ozaki, B.J. Peterson, A. Sagara, S. Sakakibara, R. Sakamoto, H. Sasao, M. Sasao, K. Sato, M. Sato, T. Seki, T. Shimozuma, M. Shoji, H. Suzuki, Y. Takeiri, K. Tanaka, K. Toi, T. Tokuzawa, K. Tsumori, I. Yamada, H. Yamada, S. Yamaguchi, M. Yokoyama, K.Y. Watanabe, T. Watari, R. Akiyama, H. Chikaraishi, K. Haba, S. Hamaguchi, S. Iima, S. Imagawa, N. Inoue, K. Iwamoto, S. Kitagawa, Y. Kubota, J. Kodaira, R. Maekawa, T. Mito, T. Nagasaka, A. Nishimura, Y. Takita, C. Takahashi, K. Takahata, K. Yamauchi, H. Tamura, T. Tsuzuki, S. Yamada, N. Yanagi, H. Yonezu, Y. Hamada, K. Matsuoka, K. Murai, K. Ohkubo, I. Ohtake, M. Okamoto, S. Sato, T. Satow, S. Sudo, S. Tanahashi, K. Yamazaki, M. Fujiwara and O. Motojima,
*An Overview of the Large Helical Device Project;* Oct 1998
(IAEA-CN-69/OV1/4)

NIFS-572 M. Fujiwara, H. Yamada, A. Ejiri, M. Emoto, H. Funaba, M. Goto, K. Ida, H. Idei, S. Inagaki, S. Kado, O. Kaneko, K. Kawahata, A. Komori, S. Kubo, R. Kumazawa, S. Masuzaki, T. Minami, J. Miyazawa, T. Morisaki, S. Morita, S. Murakami, S. Muto, T. Muto, Y. Nagayama, Y. Nakamura, H. Nakanishi, K. Narihara, K. Nishimura, N. Noda, T. Kobuchi, S. Ohdachi, N. Ohyabu, Y. Oka, M. Osakabe, T. Ozaki, B. J. Peterson, A. Sagara, S. Sakakibara, R. Sakamoto, H. Sasao, M. Sasao, K. Sato, M. Sato, T. Seki, T. Shimozuma, M. Shoji, H. Sazuki, Y. Takeiri, K. Tanaka, K. Toi, T. Tokuzawa, K. Tsumori, I. Yamada, S. Yamaguchi, M. Yokoyama, K.Y. Watanabe, T. Watari, R. Akiyama, H. Chikaraishi, K. Haba, S. Hamaguchi, M. Iima, S. Imagawa, N. Inoue, K. Iwamoto, S. Kitagawa, Y. Kubota, J. Kodaira, R. Maekawa, T. Mito, T. Nagasaka, A. Nishimura, Y. Takita, C. Takahashi, K. Takahata, K. Yamauchi, H. Tamura, T. Tsuzuki, S. Yamada, N. Yanagi, H. Yonezu, Y. Hamada, K. Matsuoka, K. Murai, K. Ohkubo, I. Ohtake, M. Okamoto, S. Sato, T. Satow, S. Sudo, S. Tanahashi, K. Yamazaki, O. Motojima and A. Iiyoshi,
*Plasma Confinement Studies in LHD;* Oct 1998
(IAEA-CN-69/EX2/3)

NIFS-573 O. Motojima, K. Akaishi, H. Chikaraishi, H. Funaba, S. Hamaguchi, S. Imagawa, S. Inagaki, N. Inoue, A. Iwamoto, S. Kitagawa, A. Komori, Y. Kubota, R. Maekawa, S. Masuzaki, T. Mito, J. Miyazawa, T. Morisaki, T. Muroga, T. Nagasaka, Y. Nakmura, A. Nishimura, K. Nishimura, N. Noda, N. Ohyabu, S. Sagara, S. Sakakibara, R. Sakamoto, S. Satoh, T. Satow, M. Shoji, H. Suzuki, K. Takahata, H. Tamura, K. Watanabe, H. Yamada, S. Yamada, S. Yamaguchi, K. Yamazaki, N. Yanagi, T. Baba, H. Hayashi, M. Iima, T. Inoue, S. Kato, T. Kato, T. Kondo, S. Moriuchi, H. Ogawa, I. Ohtake, K. Ooba, H. Sekiguchi, N. Suzuki, S. Takami, Y. Taniguchi, T. Tsuzuki, N. Yamamoto, K. Yasui, H. Yonezu, M. Fujiwara and A. Iiyoshi,
*Progress Summary of LHD Engineering Design and Construction,* Oct. 1998
(IAEA-CN-69/FT2/1)

NIFS-574 K. Toi, M. Takechi, S. Takagi, G. Matsunaga, M. Isobe, T. Kondo, M. Sasao, D.S. Darrow, K. Ohkuni, S. Ohdachi, R. Akiyama, A. Fujisawa, M. Gotoh, H. Idei, K. Ida, H. Iguchi, S. Kado, M. Kojima, S. Kubo, S. Lee, K. Matsuoka, T. Minami, S. Morita, N. Nikai, S. Nishimura, S. Okamura, M. Osakabe, A. Shimizu, Y. Shirai, C. Takahashi, K. Tanaka, T. Watari and Y. Yoshimura,
*Global MHD Modes Excited by Energetic Ions in Heliotron/Torsatron Plasmas*; Oct. 1998
(IAEA-CN-69/EXP1/19)

NIFS-575 Y. Hamada, A. Nishizawa, Y. Kawasumi, A. Fujisawa, M. Kojima, K. Narihara, K. Ida, A. Ejiri, S. Ohdachi, K. Kawahata, K. Toi, K. Sato, T. Seki, H. Iguchi, K. Adachi, S. Hidekuma, S. Hirokura, K. Iwasaki, T. Ido, R. Kumazawa, H. Kuramoto, T. Minami, L. Nomura, M. Sasao, K.N. Sato, T. Tsuzuki, I. Yamada and T. Watari,
*Potential Turbulence in Tokamak Plasmas*; Oct. 1998
(IAEA-CN-69/EXP2/14)

NIFS-576 S. Murakami, U. Gasparino, H. Idei, S. Kubo, H. Maassberg, N. Marushchenko, N. Nakajima, M. Romé and M. Okamoto,
*5D Simulation Study of Suprathermal Electron Transport in Non-Axisymmetric Plasmas*, Oct. 1998
(IAEA-CN-69/THP1/01)

NIFS-577 S. Fujiwara and T. Sato,
*Molecular Dynamics Simulation of Structure Formation of Short Chain Molecules*; Nov 1998

NIFS-578 T. Yamagishi,
*Eigenfunctions for Vlasov Equation in Multi-species Plasmas* Nov 1998

NIFS-579 M. Tanaka, A. Yu Grosberg and T. Tanaka,
*Molecular Dynamics of Strongly-Coupled Multichain Coulomb Polymers in Pure and Salt Aqueous Solutions*; Nov 1998

NIFS-580 J. Chen, N. Nakajima and M. Okamoto,
*Global Mode Analysis of Ideal MHD Modes in a Heliotron/Torsatron System: I. Mercier-unstable Equilibria*; Dec. 1998

NIFS-581 M. Tanaka, A. Yu Grosberg and T. Tanaka,
*Comparison of Multichain Coulomb Polymers in Isolated and Periodic Systems: Molecular Dynamics*

*Study;* Jan. 1999

NIFS-582 V.S. Chan and S. Murakami,
*Self-Consistent Electric Field Effect on Electron Transport of ECH Plasmas*; Feb. 1999

NIFS-583 M. Yokoyama, N. Nakajima, M. Okamoto, Y. Nakamura and M. Wakatani,
*Roles of Bumpy Field on Collisionless Particle Confinement in Helical-Axis Heliotrons*; Feb. 1999

NIFS-584 T.-H. Watanabe, T. Hayashi, T. Sato, M. Yamada and H. Ji,
*Modeling of Magnetic Island Formation in Magnetic Reconnection Experiment*; Feb. 1999

NIFS-585 R. Kumazawa, T. Mutoh, T. Seki, F. Shinpo, G. Nomura, T. Ido, T. Watari, Jean-Marie Noterdaeme and Yangping Zhao,
*Liquid Stub Tuner for Ion Cyclotron Heating*; Mar. 1999

NIFS-586 A. Sagara, M. Iima, S. Inagaki, N. Inoue, H. Suzuki, K. Tsuzuki, S. Masuzaki, J. Miyazawa, S. Morita, Y. Nakamura, N. Noda, B. Peterson, S. Sakakibara, T. Shimozuma, H. Yamada, K. Akaishi, H. Chikaraishi, H. Funaba, O. Kaneko, K. Kawahata, A. Komori, N. Ohyabu, O. Motojima, LHD Exp. Group 1, LHD Exp. Group 2,
*Wall Conditioning at the Starting Phase of LHD*; Mar. 1999

NIFS-587 T. Nakamura and T. Yabe,
*Cubic Interpolated Propagation Scheme for Solving the Hyper-Dimensional Vlasov-Poisson Equation in Phase Space*; Mar. 1999

NIFS-588 W.X. Wnag, N. Nakajima, S. Murakami and M. Okamoto,
*An Accurate $\delta f$ Method for Neoclassical Transport Calculation*; Mar. 1999

NIFS-589 K. Kishida, K. Araki, S. Kishiba and K. Suzuki,
*Local or Nonlocal? Orthonormal Divergence-free Wavelet Analysis of Nonlinear Interactions in Turbulence*, Mar. 1999

NIFS-590 K. Araki, K. Suzuki, K. Kishida and S. Kishiba,
*Multiresolution Approximation of the Vector Fields on $T^3$*; Mar. 1999

NIFS-591 K. Yamazaki, H. Yamada, K.Y.Watanabe, K. Nishimura, S. Yamaguchi, H. Nakanishi, A. Komori, H. Suzuki, T. Mito, H. Chikaraishi, K. Murai, O. Motojima and the LHD Group,
*Overview of the Large Helical Device (LHD) Control System and Its First Operation*; Apr. 1999

NIFS-592 T. Takahashi and Y. Nakao,
*Thermonuclear Reactivity of D-T Fusion Plasma with Spin-Polarized Fuel*; Apr. 1999

NIFS-593 H. Sugama,
*Damping of Toroidal Ion Temperature Gradient Modes*; Apr. 1999

NIFS-594 Xiaodong Li,
*Analysis of Crowbar Action of High Voltage DC Power Supply in the LHD ICRF System*; Apr. 1999

NIFS-595 K. Nishimura, R. Horiuchi and T. Sato,
*Drift-kink Instability Induced by Beam Ions in Field-reversed Configurations*; Apr. 1999

NIFS-596 Y. Suzuki, T-H. Watanabe, T. Sato and T. Hayashi,
*Three-dimensional Simulation Study of Compact Toroid Plasmoid Injection into Magnetized Plasmas*; Apr. 1999

NIFS-597 H. Sanuki, K. Itoh, M. Yokoyama, A. Fujisawa, K. Ida, S. Toda, S.-I. Itoh, M. Yagi and A. Fukuyama,
*Possibility of Internal Transport Barrier Formation and Electric Field Bifurcation in LHD Plasma*; May 1999

NIFS-598 S. Nakazawa, N. Nakajima, M. Okamoto and N. Ohyabu,
*One Dimensional Simulation on Stability of Detached Plasma in a Tokamak Divertor*; June 1999

NIFS-599 S. Murakami, N. Nakajima, M. Okamoto and J. Nhrenberg,
*Effect of Energetic Ion Loss on ICRF Heating Efficiency and Energy Confinement Time in Heliotrons*; June 1999

NIFS-600 R. Horiuchi and T. Sato,

*Three-Dimensional Particle Simulation of Plasma Instabilities and Collisionless Reconnection in a Current Sheet*;, June 1999

NIFS-601 W. Wang, M. Okamoto, N. Nakajima and S. Murakami,
*Collisional Transport in a Plasma with Steep Gradients*, June 1999

NIFS-602 T. Mutoh, R. Kumazawa, T. Saki, K. Saito, F. Simpo, G. Nomura, T. Watari, X. Jikang, G. Cattanei, H. Okada, K. Ohkubo, M. Sato, S. Kubo, T. Shimozuma, H. Idei, Y. Yoshimura, O. Kaneko, Y. Takeiri, M. Osakabe, Y. Oka, K. Tsumori, A. Komori, H. Yamada, K. Watanabe, S. Sakakibara, M. Shoji, R. Sakamoto, S. Inagaki, J. Miyazawa, S. Morita, K. Tanaka, B.J. Peterson, S. Murakami, T. Minami, S. Ohdachi, S. Kado, K. Narihara, H. Sasao, H. Suzuki, K. Kawahata, N. Ohyabu, Y. Nakamura, H. Funaba, S. Masuzaki, S. Muto, K. Sato, T. Morisaki, S. Sudo, Y. Nagayama, T. Watanabe, M. Sasao, K. Ida, N. Noda, K. Yamazaki, K. Akaishi, A. Sagara, K. Nishimura, T. Ozaki, K. Toi, O. Motojima, M. Fujiwara, A. Iiyoshi and LHD Exp. Group 1 and 2,
*First ICRF Heating Experiment in the Large Helical Device*; July 1999

NIFS-603 P.C. de Vries, Y. Nagayama, K. Kawahata, S. Inagaki, H. Sasao and K. Nagasaki,
*Polarization of Electron Cyclotron Emission Spectra in LHD*; July 1999

NIFS-604 W. Wang, N. Nakajima, M. Okamoto and S. Murakami,
*$\delta f$ Simulation of Ion Neoclassical Transport;* July 1999

NIFS-605 T. Hayashi, N. Mizuguchi, T. Sato and the Complexity Simulation Group,
*Numerical Simulation of Internal Reconnection Event in Spherical Tokamak*, July 1999

NIFS-606 M. Okamoto, N. Nakajima and W. Wang,
*On the Two Weighting Scheme for $\delta f$ Collisional Transport Simulation*; Aug. 1999

NIFS-607 O. Motojima, A.A. Shishkin, S. Inagaki, K.Y. Watanabe,
*Possible Control Scenario of Radial Electric Field by Loss-Cone-Particle Injection into Helical Device*; Aug. 1999

NIFS-608 R. Tanaka, T. Nakamura and T. Yabe,
*Constructing Exactly Conservative Scheme in Non-conservative Form*; Aug. 1999

NIFS-609 H. Sugama,
*Gyrokinetic Field Theory*; Aug. 1999

NIFS-610 M. Takechi, G. Matsunaga, S. Takagi, K.Ohkuni, K. Toi, M. Osakabe, M. Isobe, S. Okamura, K. Matsuoka, A. Fujisawa, H. Iguchi, S. Lee, T. Minami, K. Tanaka, Y. Yoshimura and CHS Group,
*Core Localized Toroidal Alfven Eigenmodes Destabilized By Energetic Ions in the CHS Heliotron/Torsatron*; Sep. 1999

NIFS-611 K. Ichiguchi,
*MHD Equilibrium and Stability in Heliotron Plasmas*; Sep. 1999

NIFS-612 Y. Sato, M. Yokoyama, M. Wakatani and V. D. Pusovitov,
*Complete Suppression of Pfirsch-Schluter Current in a Toroidal l=3 Stellarator*, Oct. 1999

NIFS-613 S. Wang, H. Sanuki and H. Sugama,
*Reduced Drift Kinetic Equation for Neoclassical Transport of Helical Plasmas in Ultra-low Collisionality Regime*, Oct. 1999

NIFS-614 J. Miyazawa, H. Yamada, K. Yasui, S. Kato, N., Fukumoto, M. Nagata and T. Uyama,
*Design of Spheromak Injector Using Conical Accelerator for Large Helical Device*, Nov. 1999

NIFS-615 M. Uchida, A. Fukuyama, K. Itoh, S.-I. Itoh and M. Yagi,
*Analysis of Current Diffusive Ballooning Mode in Tokamaks*, Dec. 1999

NIFS-616 M. Tanaka, A.Yu. Grosberg and T. Tanaka,
*Condensation and Swelling Behavior of Randomly Charged Multichain Polymers by Molecular Dynamics Simulations;* Dec. 1999

NIFS-617 S. Goto and S. Kida,
*Sparseness of Nonlinear Coupling*, Dec. 1999

NIFS-618 M.M. Skoric, T. Sato, A. Maluckov and M.S. Jovanovic,
*Complexity in Laser Plasma Instabilities* Dec. 1999

NIFS-619 T.-H. Watanabe, H. Sugama and T. Sato,
*Non-dissipative Kinetic Simulation and Analytical Solution of Three-mode Equations of Ion Temperature Gradient Instability*; Dec. 1999

NIFS-620 Y. Oka, Y. Takeiri, Yu.I.Belchenko, M. Hamabe, O. Kaneko, K. Tsumori, M. Osakabe, E. Asano, T. Kawamoto, R. Akiyama,
*Optimization of Cs Deposition in the 1/3 Scale Hydrogen Negative Ion Source for LHD-NBI System* ;Dec. 1999

NIFS-621 Yu.I. Belchenko, Y. Oka, O. Kaneko, Y. Takeiri, A. Krivenko, M. Osakabe, K. Tsumori, E. Asano, T. Kawamoto, R. Akiyama,
*Recovery of Cesium in the Hydrogen Negative Ion Sources*;Dec. 1999

NIFS-622 Y. Oka, O. Kaneko, K. Tsumori, Y. Takeiri, M. Osakabe, T. Kawamoto, E. Asano, and R. Akiyama,
*H- Ion Source Using a Localized Virtual Magnetic Filter in the Plasma Electrode: Type I LV Magnetic Filter:* Dec 1999

NIFS-623 M. Tanaka, S Kida, S. Yanase and G. Kawahara,
*Zero-absolute-vorticity State in a Rotating Turbulent Shear Flow*;Jan. 2000

NIFS-624 F. Leuterer, S. Kubo,
*Electron Cyclotron Current Drive at* $\omega \approx \omega_c$ *with X-mode Launched from the Low Field Side;* Feb. 2000

NIFS-625 K. Nishimura,
*Wakefield of a Charged Particulate Influenced by Emission Process of Secondary Electrons*; Mar. 2000

NIFS-626 K. Itoh, M. Yagi, S.-I. Itoh, A. Fukuyama,
*On Turbulent Transport in Burning Plasmas*,Mar 2000

NIFS-627 K. Itoh, S.-I. Itoh, L. Giannone,
*Modelling of Density Limit Phenomena in Toroidal Helical Plasmas*; Mar. 2000

NIFS-628 K. Akaishi, M. Nakasuga and Y. Funato,
*True and Measured Outgassing Rates of a Vacuum Chamber with a Reversibly Absorbed Phase*;Mar. 2000

NIFS-629 T. Yamagishi,
*Effect of Weak Dissipation on a Drift Orbit Mapping*; Mar. 2000

NIFS-630 S. Toda, S.-I. Itoh, M. Yagi, A. Fukuyama and K. Itoh,
*Spatial Structure of Compound Dither in L/H Transition*;Mar. 2000

NIFS-631 N. Ishihara and S. Kida,
*Axial and Equatorial Magnetic Dipoles Generated in a Rotating Spherical Shell;* Mar. 2000

NIFS-632 T. Kuroda, H. Sugama, R. Kanno and M. Okamoto,
*Ion Temperature Gradient Modes in Toroidal Helical Systems*; Apr. 2000

NIFS-633 V.D. Pustovitov,
*Magnetic Diagnostics: General Principles and the Problem of Reconstruction of Plasma Current and Pressure Profiles in Toroidal Systems*; Apr 2000

NIFS-634 A.B. Mikhailovskii, S.V. Konovalov, V.D Pustovitov and V.S. Tsypin,
*Mechanism of Viscosity Effect on Magnetic Island Rotation*; Apr 2000

NIFS-635 H. Naitou, T. Kuramoto, T. Kobayashi, M. Yagi, S. Tokuda and T. Matsumoto,
*Stabilization of Kinetic Internal Kink Mode by Ion Diamagnetic Effects*; Apr. 2000

NIFS-636 A. Kageyama and S. Kida,
*A Spectral Method in Spherical Coordinates with Coordinate Singularity at the Origin*; Apr. 2000

NIFS-637 R. Horiuchi, W. Pei and T. Sato,
*Collisionless Driven Reconnection in an Open System*;June 2000